ACS Energy LETTERS

http://pubs.acs.org/journal/aelccp

Uncorrelated Lithium-Ion Hopping in a Dynamic Solvent–Anion Network

Deyang Yu, Diego Troya, Andrew G. Korovich, Joshua E. Bostwick, Ralph H. Colby, and Louis A. Madsen*

Cite This: *ACS Energy Lett.* 2023, 8, 1944–1951

Read Online

ACCESS | Metrics & More | Article Recommendations | Supporting Information

ABSTRACT: **Lithium batteries rely crucially on fast charge and mass transport of Li^+ in the electrolyte. For liquid and polymer electrolytes with added lithium salts, Li^+ couples to the counter-anion to form ionic clusters that produce inefficient Li^+ transport and lead to Li dendrite formation. Quantification of Li^+ transport in glycerol–salt electrolytes via NMR experiments and MD simulations reveals a surprising Li^+-hopping mechanism. The Li^+ transference number, measured by ion-specific electrophoretic NMR, can reach 0.7, and Li^+ diffusion does not correlate with nearby ion motions, even at high salt concentration. Glycerol's high density of hydroxyl groups increases ion dissociation and slows anion diffusion, while the close proximity of hydroxyls and anions lowers local energy barriers, facilitating Li^+ hopping. This system represents a bridge between liquid and inorganic solid electrolytes, thus motivating new molecular designs for liquid and polymer electrolytes to enable the uncorrelated Li^+-hopping transport needed for fast-charging and all-solid-state batteries.**

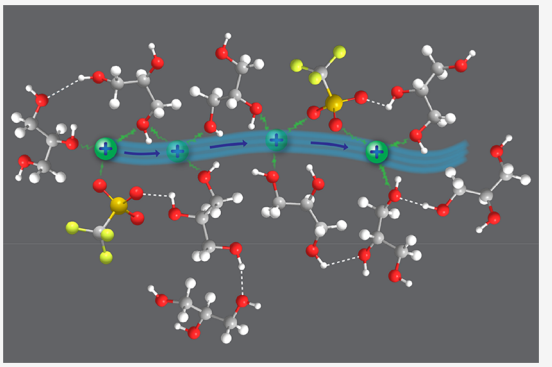

In inorganic solid electrolytes, lithium ions (Li^+) hop along favorable energetic pathways in a coordinating framework, and ionic conductivity is governed by properties such as defect formation energy, hopping energy barrier, hopping distance, and attempt frequency.[1,2] The ionic conductivity is determined primarily by Li^+, leading to the Li^+ transference number (t_{Li^+}) approaching 1. In contrast, in a typical liquid electrolyte composed of a lithium salt and solvent, lithium ions exist in solvation shells that move collectively in the so-called vehicular transport mechanism. In this paradigm, Li^+ conductivity originates from the translational motion of the solvated Li^+. Because the hydrodynamic radius of solvated Li^+ is larger than that of individual solvent molecules and (nearly always) counter-anions, Li^+ diffuses slower than both solvent molecules and anions.[3] The obtained t_{Li^+} is thus typically less than 0.4.[4] Furthermore, the formation of ion pairs and larger clusters due to strong electrostatic interactions causes the motions of Li^+ and the anions to strongly couple to each other. This not only results in a measured conductivity much lower than the conductivity calculated from diffusion coefficients but also can lead to negative t_{Li^+}.[5,6] The Li^+ transport mechanism is similar in polymer electrolytes, and the slow dynamics of polymer chain motions further reduce conductivity. Therefore, developing liquid and polymer electrolytes in which Li^+ exhibits a dominant uncorrelated hopping mechanism is highly desirable for fast-charging and all-solid-state batteries.

In traditional liquid electrolytes, solvation shell molecules are in rapid dynamic exchange with free solvent molecules.[7−9] This rapid ligand exchange implies that a Li^+ can diffuse between different locations simply by exchanging its solvating molecules. Such a ligand exchange/hopping mechanism exists in a range of highly concentrated liquid electrolytes.[10−21] However, a high salt concentration in these electrolytes introduces intense ion–ion interactions, which generally reduce conductivity. Moreover, the conductivity of "polymer-in-salt" electrolytes, the polymerized version of highly concentrated liquid electrolytes, is still not suitable for commercial applications, even after several decades of research.[22,23]

Under these circumstances, we seek electrolyte molecular structures in flexible and scalable soft materials (liquids, polymers, etc.) that allow facile Li^+-hopping transport. Here, we report a Li^+-hopping transport mechanism in a matrix of solvent–anion molecules enabled by the highly hydrogen-bonding molecule glycerol. Electrophoretic NMR and dynamic

Received: March 1, 2023
Accepted: March 9, 2023
Published: March 28, 2023

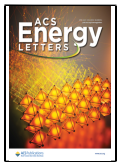

https://doi.org/10.1021/acsenergylett.3c00454
ACS Energy Lett. 2023, 8, 1944–1951

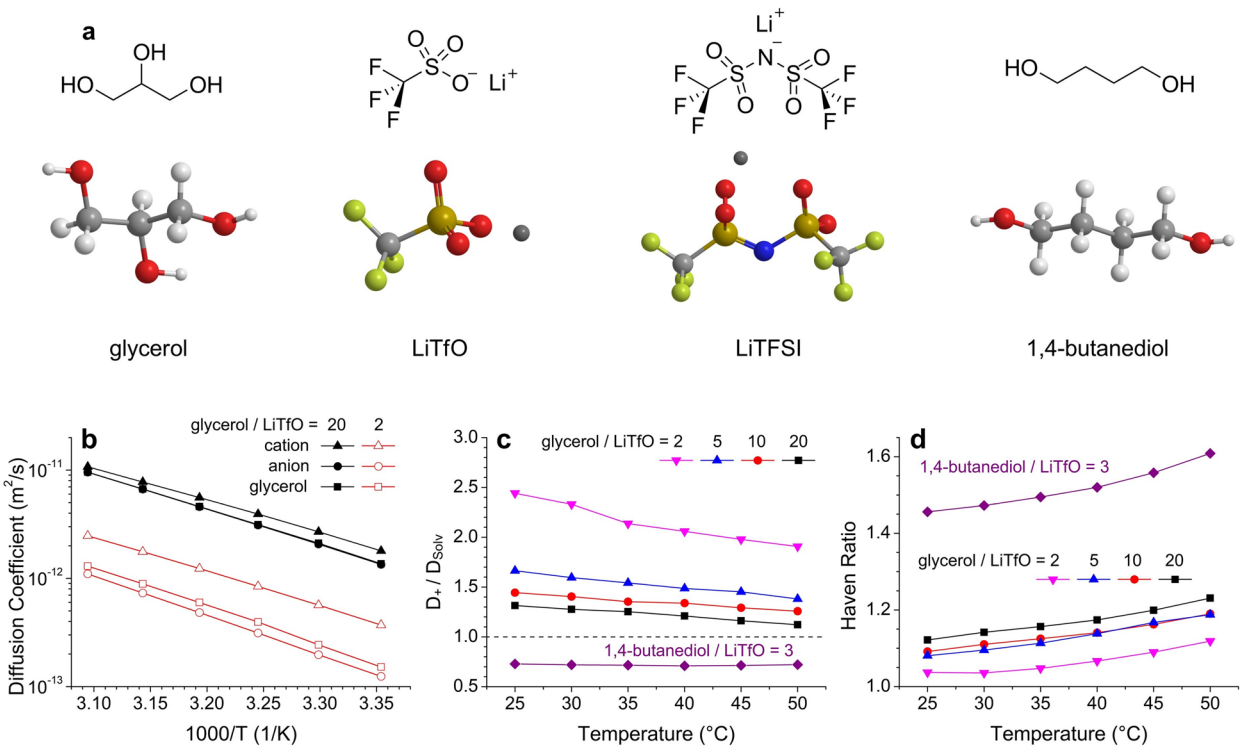

Figure 1. Diffusion coefficients and Haven ratios of binary electrolytes. (a) Chemical structures of the lithium salts and solvents. (b) Diffusion coefficients of the cation (D_+), anion (D_-), and glycerol (D_{Solv}) in glycerol−LiTfO binary solutions, where the molar ratios of glycerol and LiTfO are 20 and 2. (c) Temperature dependence of D_+/D_{Solv} ratios in glycerol−LiTfO electrolytes with various molar ratios compared to those of a mixture of 1,4-butanediol and LiTfO at molar ratio of 3. D_+/D_- ratios follow quite similar trends to D_+/D_{Solv} ratios (see Figure S1) (d) Haven ratios ($H = \sigma^{DNMR}/\sigma^{EIS}$) of all LiTfO-containing electrolytes as a function of temperature. These measurements show that Li^+ diffuses fastest in glycerol, and H of glycerol electrolytes falls below those of other non-dilute liquid electrolytes.

ion correlation analysis reveal that the Li^+ hopping is independent from the anion motions. The demonstration of such an uncorrelated hopping mechanism over a wide concentration range in these electrolytes opens the door to new molecular structures that can facilitate efficient Li^+ transport in both liquid and polymer electrolytes.

Ion and Solvent Diffusion and Conductivity. In order to comprehensively understand the transport of solvent and ions, we directly measure Li^+, counter-ion, and solvent self-diffusion (D), ionic conductivity (σ), and Li^+ and counter-ion electrophoretic mobility (μ). We then combine these quantities to draw critical conclusions about associations among ions and solvent molecules. We begin by discussing species-specific diffusion coefficients and ionic conductivity.

Figure 1b shows the temperature-dependent diffusion coefficients of all mobile species in glycerol solutions with lithium trifluoromethanesulfonate (LiTfO) salt, measured using pulsed-field-gradient (PFG) NMR diffusometry. At a molar ratio of glycerol/LiTfO = 20, the diffusion coefficients of glycerol (D_{Solv}) and TfO^- (D_-) are nearly identical and are lower than that of Li^+ (D_+), indicating that the vehicular mechanism alone cannot describe the Li^+ transport behavior in this system, even in dilute conditions. The ratios between the diffusion coefficient of Li^+ and the solvent glycerol (D_+/D_{Solv}) are 1.3 and 1.1 at 25 °C and 50 °C, respectively (Figure 1c). In such a dilute solution, D_{Solv} is dominated by molecules that have little or no interactions with the ions. At higher salt contents, both D_+/D_{Solv} and D_+/D_- increase substantially. When the molar ratio of glycerol/LiTfO = 2, D_+/D_{Solv} increases to 2.4 at 25 °C and D_+/D_- reaches 3.0 (Figure S1a). For all electrolyte solutions, D_+/D_{Solv} and D_+/D_- decrease with temperature, demonstrating that Li^+ has a lower activation energy of diffusion than the anion and the solvent, regardless of concentration. We obtain similar results with other lithium salts, such as lithium bis(trifluoromethanesulfonyl)imide (LiTFSI). Figure S2 compares the diffusion coefficients of glycerol−LiTFSI and glycerol−LiTfO solutions at the same molar ratio of 10. $TFSI^-$ shows slightly slower diffusion than TfO^- due to its larger hydrodynamic radius, but glycerol and Li^+ show no significant variation in their diffusion coefficients, strongly implying that this hydrogen-bond-dense solvent drives this behavior. In contrast, in a binary solution composed of 1,4-butanediol (which has a molar mass similar to that of glycerol but with one fewer −OH group per molecule) and LiTfO at molar ratio of 3, Li^+ diffuses slower than both the anion and the solvent, and with a typical D_+/D_{Solv} of 0.73 at 25 °C (Figure 1c and Figure S3b). The fact that Li^+ is the fastest species in glycerol solutions negates a vehicular mechanism as the sole Li^+ transport mechanism and supports the presence of significant ion-hopping, even in dilute solutions.

Figure S1b shows ionic conductivities of the glycerol electrolytes measured using electrochemical impedance spectroscopy (EIS). We performed EIS consecutively with PFG NMR diffusometry by inserting two Pd electrodes into the sample tube used for NMR measurements (Figure S4a). We thus minimize the experimental error when comparing diffusion data with conductivity. The Nernst−Einstein equation (eq 1) establishes the relationship between the ionic diffusion coefficients and conductivity in an infinitely dilute solution:

https://doi.org/10.1021/acsenergylett.3c00454
ACS Energy Lett. 2023, 8, 1944−1951

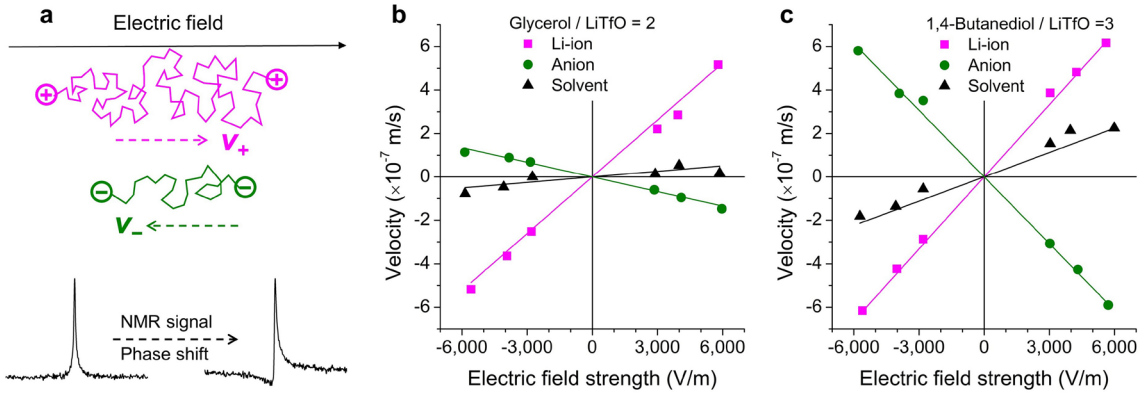

Figure 2. Electrophoretic NMR characterizes the mobility of ionic species as well as the solvent. (a) Schematic illustration of the ENMR ion migration (mobility) mechanism. Migration of species in an electric (E) field causes a phase shift of the corresponding spectral peaks in an ENMR experiment. Analyzing this phase shift for each species yields their velocities. (b, c) Velocities of cation (^{7}Li), anion (^{19}F), and solvent (^{1}H) plotted against the applied E-field strength in glycerol/LiTfO = 2 and 1,4-butanediol/LiTfO = 3. The solid lines are fits to the experimental data points, and the slope of each solid line yields the mobility (μ) of that species. Although the Li$^+$ mobility (μ_+) values in these two samples are very similar, the anion and solvent mobilities in glycerol are significantly lower relative to those of the butanediol sample, supporting a Li$^+$-hopping transport mechanism in glycerol electrolytes.

Table 1. Summary of the Main Transport Results from Consecutive Pulsed-Field-Gradient (PFG) NMR Diffusometry, Electrophoretic NMR (ENMR), and Electrochemical Impedance Spectroscopy (EIS) Measurements[a]

		Diffusion coeff. ($\times 10^{-12}$ m^2/s)			Mobility ($\times 10^{-11}$ m^2/(s·V))			Conductivity (mS/cm)			Li$^+$ transference number		Haven ratio	
Sample	T (°C)	D_+	D_-	D_{Solv}	μ_+	μ_-	μ_{Solv}	σ^{EIS}	σ^{DNMR}	σ^{ENMR}	t^{DNMR}	t^{ENMR}	H_+	H_-
Butanediol/LiTfO = 3	50	4.3	4.9	6.0	11	10	3.7	0.59	0.94	0.61	0.47	0.35	1.40	1.73
Glycerol/LiTfO = 2	50	2.5	1.1	1.3	8.7	2.3	0.85	0.49	0.55	0.47	0.69	0.72	1.02	1.76
Glycerol/LiTfO = 20	30	2.7	2.1	2.1	11	5.9	0.51	0.10	0.12	0.11	0.57	0.61	0.98	1.35
	50	11	9.6	9.6	31	24	2.2	0.38	0.46	0.35	0.53	0.52	1.24	1.44

[a]The subscripts +, −, and Solv denote cation, anion, and solvent, respectively. Solvent mobility (μ_{Solv}) is defined as the slope of the v vs E plot of the solvent molecules from ENMR The experimental errors of the diffusion coefficient and impedance measurements are <±5%. The errors of the mobility measurements are estimated to be ±15%, except for glycerol, for which the error can be 30%−50% due to the small phase shift in its measurement.

$$\sigma^{DNMR} = \frac{cF^2}{RT}(D_+ + D_-) \quad (1)$$

where σ^{DNMR} is the ionic conductivity derived from diffusion coefficients, c is the salt concentration, F is the Faraday constant, and R is the gas constant. In liquid and polymer electrolytes, σ^{DNMR} is typically larger than the ionic conductivity measured by EIS (σ^{EIS}) due to the presence of dynamic ion−ion interactions.[24−28] Thus, the so-called Haven ratio, $H = \sigma^{DNMR}/\sigma^{EIS}$, is larger than 1. For instance, H for ionic liquids is typically 1.3−2,[29−31] and for a highly concentrated 3 mol/L LiTFSI in sulfolane electrolyte H is 1.4.[32] H for LiTFSI in a variety of organic solvents for battery applications ranges from 1.5 to 10.[3] The 1,4-butanediol electrolyte solution in this work exhibits H similar to those of ionic liquids (1.46 at 25 °C, Figure 1d). However, H values for the glycerol−salt electrolytes are near unity (from 1.12 to 1.04), with the additional surprise that they decrease with increasing salt concentration.

We hypothesize that the presence of Li$^+$ hopping and low Haven ratios in these electrolytes arises from the high density of hydroxyl groups on glycerol, which establish strong multi-contact H-bonds with the anion. This strongly contrasts with the behaviors of essentially all commonly studied electrolyte solvents, such as organic carbonates, esters, and ethers. Figure S5 shows the ^{1}H NMR spectrum of glycerol as a function of salt concentration. With increasing salt concentration, glycerol's methine and methylene groups (−C**H**− and −C**H**$_2$−) shift to lower field on account of the deshielding effect when the oxygens on the −OH groups of glycerol solvate Li$^+$. Meanwhile, the −O**H** nuclei shift to higher field by the shielding effect of hydrogen-bonded TfO$^-$ ions. In short, the high density of hydroxyl groups in glycerol provides strong interactions with both ions, which effectively screens cation−anion interactions.

The ability of glycerol to establish multi-contact hydrogen bonds with both the anions and other glycerol molecules gives rise to the slow diffusion of glycerol and TfO$^-$ and furthermore enables glycerol and TfO$^-$ to form a dynamic, slow-diffusing, and percolating network through which Li$^+$ can transport via a ligand-exchange/hopping mechanism. We note that individual −O**H**···Li$^+$ interactions should be very strong due to the high polarity of the −OH group, and yet Li$^+$ can demonstrate such a hopping mechanism primarily because of the high number density and close spacing of −OH groups. This close spacing yields a small average well depth (or level of corrugation) in the local potential energy surface for Li$^+$ transport, as in an inorganic Li$^+$ conductor. In contrast, 1,4-butanediol has a notably reduced hydroxyl group density (two hydroxyl groups on four carbon atoms), causing a larger Li$^+$-hopping distance and thus higher average energy barriers. Hence, Li$^+$ in 1,4-

https://doi.org/10.1021/acsenergylett.3c00454
ACS Energy Lett. 2023, 8, 1944−1951

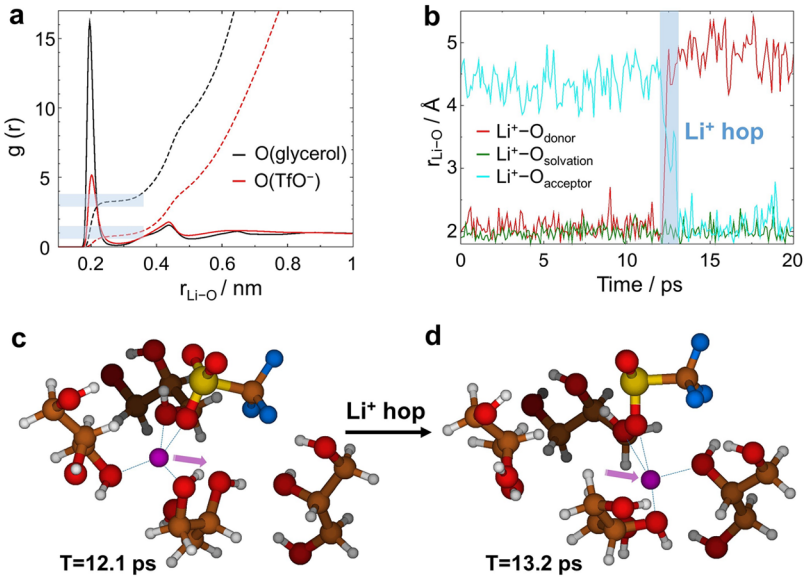

Figure 3. Lithium-ion hopping in MD simulations. (a) Radial distribution functions (rdfs) of the O atoms of glycerol and TfO^- to Li^+ at 50 °C in glycerol/LiTfO = 2. Dashed lines represent the cumulative coordination number, and shaded bars highlight rdf plateaus at ∼1 and 3 O−Li coordination numbers. (b) Internuclear distances between a Li^+ and representative O atoms in the inner solvation shell, highlighting the ligand exchange of Li^+ in a hop between donor (red trace) and acceptor (cyan) molecules. A spectator Li^+−O distance is shown for reference (green trace). (c, d) Snapshots of the inner solvation shell of the Li^+ before and after a hopping event.

butanediol, like traditional Li^+ electrolytes, forms solvated structures whose diffusion is dominated by the vehicular mechanism.

***E*-Field-Driven Mobilities of Li^+ and Counter-ions.** We now reveal how the faster diffusion of Li^+ compared to the anion in glycerol electrolytes reflects its contribution to the overall ionic conductivity via electrophoretic NMR (ENMR). Due to its robust capability to directly measure the mobility (driven motion) of separate ionic species in an electric (E) field, ENMR is emerging as an important tool in the study of electrolytes.[18,33−39] The migration of ions in the E-field leads to a phase shift of the NMR signal in ENMR (Figure 2a and Figure S6) and equates to a 1D velocity measurement (as in MR angiography).[40] By converting the phase shift into ion velocity, we obtain the mobility (μ) from the slope of a velocity (v) vs electric field strength (E) plot. See the Experimental Section in the Supporting Information for more details. Figure 2b,c shows the v vs E plots of the cation (^{7}Li), anion (^{19}F), and solvent (^{1}H) in the glycerol/LiTfO = 2 sample and the 1,4-butanediol/LiTfO = 3 sample. From Figure 2b, we can see that in the glycerol/LiTfO = 2 sample Li^+ and TfO^- migrate in opposite directions, and the Li^+ mobility in the laboratory frame (μ_+) is more than 3× higher than that of the anion (μ_-). The glycerol−Li^+ and glycerol−anion interactions apply drag to the glycerol molecules in opposite directions. Overall, glycerol slowly migrates in the same direction as Li^+, and we can assign glycerol a laboratory frame mobility μ_{Solv}, which is only 10% of the Li^+ mobility, μ_+ (Table 1). In contrast, μ_+ and μ_- in the 1,4-butanediol/LiTfO = 3 sample are nearly equal, and μ_{Solv} is 34% of μ_+ (Figure 2c and Table 1). We note that for "solvate" ionic liquid systems composed of equimolar tetraglyme and a lithium salt (either LiTFSI or $LiBF_4$), where a stable, long-lived Li^+/solvent complex is formed,[41,42] Li^+ migration is purely vehicular, and the mobilities of the solvent and cation are identical.[43] The remarkably higher μ_+/μ_{Solv} ratio for glycerol electrolytes compared to 1,4-butanediol represents compelling additional evidence for significant Li^+-hopping transport in glycerol electrolytes.

Because the ionic velocities measured directly from ENMR are relative to the reference frame of the NMR probe, the mobility obtained from the slope of v vs E plot can be regarded as a laboratory-frame mobility. Timachova et al. argued that the ionic velocities relative to the solvent ($v_+ - v_{Solv}$ and $v_- - v_{Solv}$) should be used to calculate the transference number.[36] Since we can measure the mobility of the neutral solvent, the lithium-ion transference number becomes

$$t^{ENMR} = \frac{\mu_+ - \mu_{Solv}}{(\mu_+ - \mu_{Solv}) + (\mu_- + \mu_{Solv})} \quad (2)$$

Additionally, the net ionic conductivity obtained from ENMR is

$$\sigma^{ENMR} = cF(\mu_+ + \mu_-) \quad (3)$$

From Table 1 and Table S1, we can see that σ^{ENMR} agrees with σ^{EIS} to well within the error for all samples. Remarkably, we also see general agreement between the lithium-ion transference numbers obtained from ENMR and from the diffusion coefficients ($t^{DNMR} = D_+/(D_+ + D_-)$). The only exception is the butanediol solution, for which t^{ENMR} is much lower than t^{DNMR}. This results from the high laboratory-frame mobility of the butanediol solvent molecules. The decrease of Li^+ transference number with temperature, again, originates from a slightly lower transport activation energy for the Li^+ compared to that for TfO^-. The ENMR results confirm that Li^+ is much more mobile in an applied E-field than the anion for glycerol electrolytes, leading to t^{ENMR} ranging from 0.52 to 0.72, and with the highest values at lower temperature and/or higher Li^+ concentration.

In the above analysis of diffusion and conductivity, we observe relatively low H values for the glycerol electrolytes (Figure 1d). By combining the mobilities of the cation and anion with their diffusion coefficients, we can also determine

https://doi.org/10.1021/acsenergylett.3c00454
ACS Energy Lett. 2023, 8, 1944−1951

separate cation (H_+) and anion (H_-) Haven ratios (Table 1 and S1):

$$H_+ = \frac{D_+F}{\mu_+RT} \quad \text{and} \quad H_- = \frac{D_-F}{\mu_-RT} \tag{4}$$

On the anion side, H_- ranges from 1.3 to 1.8 for the glycerol electrolytes and shows no difference between the 1,4-butanediol and the glycerol/LiTfO = 2 samples at 50 °C. However, in general, for the glycerol electrolytes $H_+ = 1$ within errors at high salt concentration or low temperature, providing the striking result that the efficiency of Li^+ diffusive mass transport that results in charge transport is 100% according to the Nernst−Einstein equation. In other words, Li^+ migrates independently from its counter-anion, even under highly concentrated conditions.

Molecular Dynamics Simulations. MD simulations further reveal rich atomistic details of the ion-hopping mechanism advanced by the experiments. MD simulations of glycerol−LiTfO binary solutions capture the measured enhanced diffusion of Li^+ with respect to the solvent and the depressed diffusion of TfO^- (e.g., $D_+/D_{Solv} = 3.35$ and $D_{Solv}/D_- = 1.07$ at 50 °C for glycerol/LiTfO = 2). Simulated Li^+ transference numbers are also close to experimental values (Table S2), inspiring confidence in the ensuing analysis of solvent/ion dynamics. Radial distribution functions (rdfs) of the distance between Li^+ and the center of mass of glycerol and TfO^- reveal that, at this molar ratio of 2, the solvation shell of Li^+ involves ca. 3 glycerol molecules and 1 TfO^- counter-ion on average (Figure S7a). Analysis of the Li−O atom rdfs (Figure 3a) indicates that the approximately tetrahedral inner solvation shell of the cation involves 3.2 Li^+−O direct contacts with the solvent O atoms, while 0.8 direct contacts occur between Li^+ and the O atoms of TfO^- on average. In the less concentrated glycerol/LiTfO = 5 electrolyte (Figure S8), glycerol forms virtually all of the solvation shell, contributing 3.8 Li^+−O contacts, with TfO^- showing only 0.2 contacts on average. These results substantiate the ability of the highly hydrogen-bonding glycerol molecule to cleanly separate Li^+ from the counter-ion over a wide range of concentration.

Trajectory analysis corroborates the hopping diffusion mechanism of Li^+ through the dynamic network of solvent and anion hypothesized experimentally. Inspection of the Li^+ Cartesian coordinates as a function of time shows that the diffusion of Li^+ is characterized by extremely fast (~1 ps) hops of significant distance (<4.2 Å) between adjacent sites in the network. The hops occur between a lithium-donor ligand, initially solvating Li^+ through a short Li−O contact, and an acceptor ligand, initially not in the inner solvation shell (Figure 3b−d). The rest of the Li^+-solvating species not exchanged in the Li^+ hops perform a supporting role by dynamically adapting to the quick change in Li^+ location. Li^+ ions experience such hops very frequently (hops longer than 1 Å occur, on average, every 200 ps at 50 °C for glycerol/LiTfO = 2). Many of these Li^+ hops correspond to frustrated attempts to diffuse through the anion/solvent network, and Li^+ returns to its original location shortly after hopping. However, a few hops (4.6% of the total at 50 °C for glycerol/LiTfO = 2) are productive for permanently advancing the ions through the network within the analysis window of 9 ns. Further analyses of hop length, time, and frequency are presented in Hop Analysis in Supporting Information. Supplementary Videos 1, 2, and 3 show representative Li^+-hop events.

Dynamic Ion Correlation Analysis. We now further analyze Li^+ transport behavior by considering dynamic ion correlations. In the framework of the Onsager reciprocal relations combined with linear response theory, the overall ionic conductivity can be written as

$$\sigma = \sigma_{++} + \sigma_{--} - 2\sigma_{+-} \tag{5}$$

where σ_{++}, σ_{--}, and σ_{+-} are the Onsager transport coefficients.[44−47] The coefficients σ_{++} and σ_{--} can be further split into self and distinct terms:

$$\sigma = \sigma_+^{self} + \sigma_{++}^{distinct} + \sigma_-^{self} + \sigma_{--}^{distinct} - 2\sigma_{+-} \tag{6}$$

The self terms relate to the diffusion coefficients via the Nernst−Einstein equation:

$$\sigma_+^{self} = c_+D_+\frac{F^2}{RT} \quad \text{and} \quad \sigma_-^{self} = c_-D_-\frac{F^2}{RT} \tag{7}$$

and the distinct terms $\sigma_{++}^{distinct}$, $\sigma_{--}^{distinct}$, and σ_{+-} describe the dynamic cation−cation, anion−anion, and cation−anion directional correlations.[45] When the motions of two species correlate (the species move in the same direction), the sign of the corresponding distinct term is positive, and when their motions anti-correlate, the sign becomes negative (see Figure S9 for additional discussion). These quantities are all defined in the laboratory frame.[48] The mobilities measured from ENMR relate to the distinct terms by

$$c_+\mu_+F = \sigma_+^{self} + \sigma_{++}^{distinct} - \sigma_{+-} \quad \text{and}$$
$$c_-\mu_-F = \sigma_-^{self} + \sigma_{--}^{distinct} - \sigma_{+-} \tag{8}$$

Thus, the difference between directly measured mobilities (ENMR) and mobilities predicted from diffusion coefficients (DNMR) arises from the dynamic directional correlations between cation−cation, anion−anion, and cation−anion.

We now use this correlation formalism to explore implications for directional ion motions in the studied electrolytes. Based on eqs 7 and 8, we can calculate σ_+^{self}/σ, σ_-^{self}/σ, $(\sigma_{++}^{distinct} - \sigma_{+-})/\sigma$, and $(\sigma_{--}^{distinct} - \sigma_{+-})/\sigma$ using measured diffusion coefficients and mobilities of the ions. The results for two glycerol electrolytes (glycerol/LiTfO = 20 and 2) and the butanediol electrolyte are shown in Figure S10. For the low-concentration (glycerol/LiTfO = 20) electrolyte, $(\sigma_{++}^{distinct} - \sigma_{+-})/\sigma$ is only 0.017 at 30 °C. Considering the low salt concentration ($c = c_+ = c_- = 0.66$ mol/L) and high dielectric constant of glycerol, σ_{+-}/σ should be negligible. Thus, $\sigma_{++}^{distinct}/\sigma = \sigma_{+-}/\sigma = 0$ within experimental error, and the direction of Li^+ hopping is not correlated to other ions nearby. When the temperature is increased to 50 °C, $(\sigma_{++}^{distinct} - \sigma_{+-})/\sigma$ drops to −0.13. We attribute this variation to the disruption of the glycerol−anion network under dilute conditions with temperature, which is also shown by the decrease of D_+/D_{Solv} and D_+/D_- from 30 °C to 50 °C. For the butanediol electrolyte, $(\sigma_{++}^{distinct} - \sigma_{+-})/\sigma$ takes a lower value of −0.21. These negative values of $(\sigma_{++}^{distinct} - \sigma_{+-})/\sigma$ highlight the role of electrostatic interactions in making the $\sigma_{++}^{distinct}/\sigma$ term negative and the σ_{+-}/σ term positive. For the highly concentrated electrolyte, glycerol/LiTfO = 2, the term $(\sigma_{++}^{distinct} - \sigma_{+-})/\sigma$ surprisingly also equals zero within error (−0.015) at 50 °C, indicating that both $\sigma_{++}^{distinct}/\sigma$ and σ_{+-}/σ have small amplitudes, and this result is supported by the MD simulations (Figure S11). Thus, the slow-diffusing dynamic glycerol−anion network appears to not only facilitate Li^+ hopping but also

https://doi.org/10.1021/acsenergylett.3c00454
ACS Energy Lett. 2023, 8, 1944−1951

greatly reduce directional cation−cation and cation−anion dynamic correlations.

In conclusion, through consecutive measurements of the ionic conductivity, diffusion coefficients, and mobilities, and in combination with MD simulations, we show that Li^+ exhibits fast and anion-decoupled transport in glycerol−lithium salt electrolytes. Li^+ transports via fast (∼1 ps) hops of <4.2 Å through a slow-diffusing solvent−anion network. Specifically, we observe the following: (1) the diffusion coefficient of Li^+ is substantially higher than those of the glycerol solvent and the counter-anion, even in dilute solution with a solvent/salt molar ratio of 20; (2) the overall solution Haven ratios are surprisingly low, approaching unity for a concentrated solution with a glycerol/LiTfO molar ratio of 2; (3) the Li^+ transference number is always >0.5, and can reach 0.7 at lower temperature and/or at higher salt content; (4) the Li^+-specific Haven ratio equals 1 for nearly all studied glycerol solutions (at lower temperature or at higher salt content), signifying 100% efficiency for converting Li^+ diffusive mass transport to driven charge transport and demonstrating ion-uncorrelated Li^+ motions; and (5) MD simulations corroborate the enhanced Li^+ transport determined experimentally and provide additional support for a hopping mechanism through a slow-diffusing dynamic network formed by glycerol and TfO^-. These salt−glycerol electrolytes bridge phenomena observed in liquid electrolytes and inorganic solid electrolytes and motivate new explorations of molecular structures for electrolytes formed from soft materials. Although glycerol is a protic solvent, we cannot exclude its application in lithium batteries by, for example, depositing artificial protecting layers on electrodes and/or further reducing its fluidity by increasing the chain length (threitol, arabitol, sorbitol, and other polyalcohols), especially considering the developments in water-in-salt electrolytes and poly(vinyl alcohol)-based polymer electrolytes.[49,50] In addition, this work can stimulate electrolyte research for applications beyond lithium batteries, such as supercapacitors and zinc batteries, where protic solvents face less stringent electrochemical challenges. This study thus dramatically widens the design parameter space available for advanced liquid and polymer battery electrolytes.

■ ASSOCIATED CONTENT

Supporting Information

The Supporting Information is available free of charge at https://pubs.acs.org/doi/10.1021/acsenergylett.3c00454.

Experimental section, extra experimental data of the diffusion coefficients of glycerol and 1,4-butanediol electrolytes, image of ENMR setup, impedance spectra, ^1H NMR spectra and chemical shift analysis, schematic illustration of diffusion and electrophoretic NMR mechanisms, schematic illustration of ion−ion correlations, extra radial distribution function plots of the glycerol electrolyte, and hop analysis (PDF)

Lithium-ion hopping video 1 (MOV)

Lithium-ion hopping video 2 (MOV)

Lithium-ion hopping video 3 (MOV)

■ AUTHOR INFORMATION

Corresponding Author

Louis A. Madsen − *Department of Chemistry, Virginia Polytechnic Institute and State University, Blacksburg, Virginia 24061, United States; Macromolecules Innovation Institute, Virginia Polytechnic Institute and State University, Blacksburg, Virginia 24061, United States;* orcid.org/0000-0003-4588-5183; Email: lmadsen@vt.edu

Authors

Deyang Yu − *Department of Chemistry, Virginia Polytechnic Institute and State University, Blacksburg, Virginia 24061, United States; Macromolecules Innovation Institute, Virginia Polytechnic Institute and State University, Blacksburg, Virginia 24061, United States;* orcid.org/0000-0003-0587-1211

Diego Troya − *Department of Chemistry, Virginia Polytechnic Institute and State University, Blacksburg, Virginia 24061, United States; Macromolecules Innovation Institute, Virginia Polytechnic Institute and State University, Blacksburg, Virginia 24061, United States;* orcid.org/0000-0003-4971-4998

Andrew G. Korovich − *Department of Chemistry, Virginia Polytechnic Institute and State University, Blacksburg, Virginia 24061, United States;* orcid.org/0000-0003-3736-1523

Joshua E. Bostwick − *Department of Materials Science and Engineering, Pennsylvania State University, University Park, Pennsylvania 16802, United States;* orcid.org/0000-0002-0640-5223

Ralph H. Colby − *Department of Materials Science and Engineering, Pennsylvania State University, University Park, Pennsylvania 16802, United States; Materials Research Institute, Pennsylvania State University, University Park, Pennsylvania 16802, United States;* orcid.org/0000-0002-5492-6189

Complete contact information is available at: https://pubs.acs.org/10.1021/acsenergylett.3c00454

Author Contributions

D.Y. conceived the idea. D.Y. and L.A.M. designed this work. D.T. performed the MD simulations. D.Y. prepared the samples and conducted the ionic conductivity and diffusion measurements. D.Y. and A.G.K. conducted the electrophoretic NMR measurements. D.Y., D.T., and L.A.M. wrote the manuscript. J.E.B. and R.H.C. participated in data analysis and manuscript writing. All authors contributed to data analysis and manuscript editing.

Notes

The authors declare no competing financial interest.

■ ACKNOWLEDGMENTS

This material is based upon work supported by the U.S. Department of Energy's Office of Energy Efficiency and Renewable Energy (EERE) under award No. DE-EE0008860. This research was also supported in part by the National Science Foundation under Award DMR 1810194. The authors gratefully acknowledge Prof. Rui Qiao at Virginia Tech for beneficial discussions.

■ REFERENCES

(1) Famprikis, T.; Canepa, P.; Dawson, J. A.; Islam, M. S.; Masquelier, C. Fundamentals of inorganic solid-state electrolytes for batteries. *Nat. Mater.* **2019**, *18* (12), 1278−1291.

(2) Wang, Y.; Richards, W. D.; Ong, S. P.; Miara, L. J.; Kim, J. C.; Mo, Y.; Ceder, G. Design principles for solid-state lithium superionic conductors. *Nat. Mater.* **2015**, *14* (10), 1026−1031.

(3) Hayamizu, K.; Aihara, Y.; Arai, S.; Martinez, C. G. Pulse-Gradient Spin-Echo 1H, 7Li, and 19F NMR Diffusion and Ionic Conductivity Measurements of 14 Organic Electrolytes Containing LiN(SO2CF3)2. *J. Phys. Chem. B* **1999**, *103* (3), 519−524.
(4) Xu, K. Nonaqueous Liquid Electrolytes for Lithium-Based Rechargeable Batteries. *Chem. Rev.* **2004**, *104* (10), 4303−4418.
(5) Gouverneur, M.; Schmidt, F.; Schönhoff, M. Negative effective Li transference numbers in Li salt/ionic liquid mixtures: does Li drift in the "Wrong" direction? *Phys. Chem. Chem. Phys.* **2018**, *20* (11), 7470−7478.
(6) Villaluenga, I.; Pesko, D. M.; Timachova, K.; Feng, Z.; Newman, J.; Srinivasan, V.; Balsara, N. P. Negative Stefan-Maxwell Diffusion Coefficients and Complete Electrochemical Transport Characterization of Homopolymer and Block Copolymer Electrolytes. *J. Electrochem. Soc.* **2018**, *165* (11), A2766−A2773.
(7) Lee, K.-K.; Park, K.; Lee, H.; Noh, Y.; Kossowska, D.; Kwak, K.; Cho, M. Ultrafast fluxional exchange dynamics in electrolyte solvation sheath of lithium ion battery. *Nat. Commun.* **2017**, *8* (1), 14658.
(8) Seo, D. M.; Borodin, O.; Balogh, D.; O'Connell, M.; Ly, Q.; Han, S.-D.; Passerini, S.; Henderson, W. A. Electrolyte Solvation and Ionic Association III. Acetonitrile-Lithium Salt Mixtures−Transport Properties. *J. Electrochem. Soc.* **2013**, *160* (8), A1061−A1070.
(9) Chen, X.; Kuroda, D. G. Molecular motions of acetonitrile molecules in the solvation shell of lithium ions. *J. Chem. Phys.* **2020**, *153* (16), 164502.
(10) Dokko, K.; Watanabe, D.; Ugata, Y.; Thomas, M. L.; Tsuzuki, S.; Shinoda, W.; Hashimoto, K.; Ueno, K.; Umebayashi, Y.; Watanabe, M. Direct Evidence for Li Ion Hopping Conduction in Highly Concentrated Sulfolane-Based Liquid Electrolytes. *J. Phys. Chem. B* **2018**, *122* (47), 10736−10745.
(11) Ugata, Y.; Sasagawa, S.; Tatara, R.; Ueno, K.; Watanabe, M.; Dokko, K. Structural Effects of Solvents on Li-Ion-Hopping Conduction in Highly Concentrated LiBF4/Sulfone Solutions. *J. Phys. Chem. B* **2021**, *125* (24), 6600−6608.
(12) Kondou, S.; Thomas, M. L.; Mandai, T.; Ueno, K.; Dokko, K.; Watanabe, M. Ionic transport in highly concentrated lithium bis(fluorosulfonyl)amide electrolytes with keto ester solvents: structural implications for ion hopping conduction in liquid electrolytes. *Phys. Chem. Chem. Phys.* **2019**, *21* (9), 5097−5105.
(13) Ugata, Y.; Thomas, M. L.; Mandai, T.; Ueno, K.; Dokko, K.; Watanabe, M. Li-ion hopping conduction in highly concentrated lithium bis(fluorosulfonyl)amide/dinitrile liquid electrolytes. *Phys. Chem. Chem. Phys.* **2019**, *21* (19), 9759−9768.
(14) Franko, C. J.; Yim, C.-H.; Årén, F.; Åvall, G.; Whitfield, P. S.; Johansson, P.; Abu-Lebdeh, Y. A.; Goward, G. R. Concentration Dependent Solution Structure and Transport Mechanism in High Voltage LiTFSI−Adiponitrile Electrolytes. *J. Electrochem. Soc.* **2020**, *167* (16), 160532.
(15) Kitada, A.; Kawata, K.; Shimizu, M.; Saimura, M.; Nagata, T.; Katahira, M.; Fukami, K.; Murase, K. Ligand Exchange Conduction of Lithium Ion in a Pentaglyme-Lithium Bis(trifluoromethylsulfonyl)-amide Super-Concentrated Electrolyte. *J. Electrochem. Soc.* **2021**, *168* (1), 016506.
(16) Galle Kankanamge, S. R.; Kuroda, D. G. Molecular Structure, Chemical Exchange, and Conductivity Mechanism of High Concentration LiTFSI Electrolytes. *J. Phys. Chem. B* **2020**, *124* (10), 1965−1977.
(17) Chen, F.; Forsyth, M. Elucidation of transport mechanism and enhanced alkali ion transference numbers in mixed alkali metal−organic ionic molten salts. *Phys. Chem. Chem. Phys.* **2016**, *18* (28), 19336−19344.
(18) Brinkkötter, M.; Mariani, A.; Jeong, S.; Passerini, S.; Schönhoff, M. Ionic Liquid in Li Salt Electrolyte: Modifying the Li+ Transport Mechanism by Coordination to an Asymmetric Anion. *Adv. Energy Sustainability Res.* **2021**, *2* (2), 2000078.
(19) Yim, C.-H.; Tam, J.; Soboleski, H.; Abu-Lebdeh, Y. On the Correlation between Free Volume, Phase Diagram and Ionic Conductivity of Aqueous and Non-Aqueous Lithium Battery Electrolyte Solutions over a Wide Concentration Range. *J. Electrochem. Soc.* **2017**, *164* (6), A1002−A1011.
(20) Andersson, R.; Årén, F.; Franco, A. A.; Johansson, P. Ion Transport Mechanisms via Time-Dependent Local Structure and Dynamics in Highly Concentrated Electrolytes. *J. Electrochem. Soc.* **2020**, *167* (14), 140537.
(21) Borodin, O.; Smith, G. D.; Henderson, W. Li+ Cation Environment, Transport, and Mechanical Properties of the LiTFSI Doped N-Methyl-N-alkylpyrrolidinium+TFSI- Ionic Liquids. *J. Phys. Chem. B* **2006**, *110* (34), 16879−16886.
(22) Angell, C. A. Concepts and conflicts in polymer electrolytes: The search for ion mobility. *Electrochim. Acta* **2019**, *313*, 205−210.
(23) Angell, C. A.; Liu, C.; Sanchez, E. Rubbery solid electrolytes with dominant cationic transport and high ambient conductivity. *Nature* **1993**, *362*, 137.
(24) Aihara, Y.; Sugimoto, K.; Price, W. S.; Hayamizu, K. Ionic conduction and self-diffusion near infinitesimal concentration in lithium salt-organic solvent electrolytes. *J. Chem. Phys.* **2000**, *113* (5), 1981−1991.
(25) Bocharova, V.; Sokolov, A. P. Perspectives for Polymer Electrolytes: A View from Fundamentals of Ionic Conductivity. *Macromolecules* **2020**, *53* (11), 4141−4157.
(26) Oldiges, K.; Diddens, D.; Ebrahiminia, M.; Hooper, J. B.; Cekic-Laskovic, I.; Heuer, A.; Bedrov, D.; Winter, M.; Brunklaus, G. Understanding transport mechanisms in ionic liquid/carbonate solvent electrolyte blends. *Phys. Chem. Chem. Phys.* **2018**, *20* (24), 16579−16591.
(27) Hayamizu, K. Temperature Dependence of Self-Diffusion Coefficients of Ions and Solvents in Ethylene Carbonate, Propylene Carbonate, and Diethyl Carbonate Single Solutions and Ethylene Carbonate + Diethyl Carbonate Binary Solutions of LiPF6 Studied by NMR. *J. Chem. Eng. Data* **2012**, *57* (7), 2012−2017.
(28) Hayamizu, K.; Aihara, Y. Ion and solvent diffusion and ion conduction of PC-DEC and PC-DME binary solvent electrolytes of LiN(SO2CF3)2. *Electrochim. Acta* **2004**, *49* (20), 3397−3402.
(29) Tokuda, H.; Hayamizu, K.; Ishii, K.; Susan, M. A. B. H.; Watanabe, M. Physicochemical Properties and Structures of Room Temperature Ionic Liquids. 1. Variation of Anionic Species. *J. Phys. Chem. B* **2004**, *108* (42), 16593−16600.
(30) Tokuda, H.; Hayamizu, K.; Ishii, K.; Susan, M. A. B. H.; Watanabe, M. Physicochemical Properties and Structures of Room Temperature Ionic Liquids. 2. Variation of Alkyl Chain Length in Imidazolium Cation. *J. Phys. Chem. B* **2005**, *109* (13), 6103−6110.
(31) Tokuda, H.; Ishii, K.; Susan, M. A. B. H.; Tsuzuki, S.; Hayamizu, K.; Watanabe, M. Physicochemical Properties and Structures of Room-Temperature Ionic Liquids. 3. Variation of Cationic Structures. *J. Phys. Chem. B* **2006**, *110* (6), 2833−2839.
(32) Nakanishi, A.; Ueno, K.; Watanabe, D.; Ugata, Y.; Matsumae, Y.; Liu, J.; Thomas, M. L.; Dokko, K.; Watanabe, M. Sulfolane-Based Highly Concentrated Electrolytes of Lithium Bis-(trifluoromethanesulfonyl)amide: Ionic Transport, Li-Ion Coordination, and Li−S Battery Performance. *J. Phys. Chem. C* **2019**, *123* (23), 14229−14238.
(33) Zhang, Z. Y.; Madsen, L. A. Observation of separate cation and anion electrophoretic mobilities in pure ionic liquids. *J. Chem. Phys.* **2014**, *140* (8), 084204.
(34) Gouverneur, M.; Kopp, J.; van Wüllen, L.; Schönhoff, M. Direct determination of ionic transference numbers in ionic liquids by electrophoretic NMR. *Phys. Chem. Chem. Phys.* **2015**, *17* (45), 30680−30686.
(35) Pfeifer, S.; Ackermann, F.; Sälzer, F.; Schönhoff, M.; Roling, B. Quantification of cation−cation, anion−anion and cation−anion correlations in Li salt/glyme mixtures by combining very-low-frequency impedance spectroscopy with diffusion and electrophoretic NMR. *Phys. Chem. Chem. Phys.* **2021**, *23* (1), 628−640.
(36) Timachova, K.; Newman, J.; Balsara, N. P. Theoretical Interpretation of Ion Velocities in Concentrated Electrolytes Measured by Electrophoretic NMR. *J. Electrochem. Soc.* **2019**, *166* (2), A264−A267.

https://doi.org/10.1021/acsenergylett.3c00454
ACS Energy Lett. 2023, 8, 1944−1951

(37) Fang, Y.; Yushmanov, P. V.; Furó, I. Improved accuracy and precision in electrophoretic NMR experiments. Current control and sample cell design. *J. Magn. Reson.* **2020**, *318*, 106796.
(38) Nürnberg, P.; Atik, J.; Borodin, O.; Winter, M.; Paillard, E.; Schönhoff, M. Superionicity in Ionic-Liquid-Based Electrolytes Induced by Positive Ion−Ion Correlations. *J. Am. Chem. Soc.* **2022**, *144* (10), 4657−4666.
(39) Simons, T. J.; Bayley, P. M.; Zhang, Z.; Howlett, P. C.; MacFarlane, D. R.; Madsen, L. A.; Forsyth, M. Influence of Zn2+ and Water on the Transport Properties of a Pyrrolidinium Dicyanamide Ionic Liquid. *J. Phys. Chem. B* **2014**, *118* (18), 4895−4905.
(40) Bryant, D. J.; Payne, J. A.; Firmin, D. N.; Longmore, D. B. Measurement of Flow with NMR Imaging Using a Gradient Pulse and Phase Difference Technique. *J. Comput. Assist. Tomogr* **1984**, *8* (4), 588−593.
(41) Ueno, K.; Yoshida, K.; Tsuchiya, M.; Tachikawa, N.; Dokko, K.; Watanabe, M. Glyme−Lithium Salt Equimolar Molten Mixtures: Concentrated Solutions or Solvate Ionic Liquids? *J. Phys. Chem. B* **2012**, *116* (36), 11323−11331.
(42) Watanabe, M.; Thomas, M. L.; Zhang, S.; Ueno, K.; Yasuda, T.; Dokko, K. Application of Ionic Liquids to Energy Storage and Conversion Materials and Devices. *Chem. Rev.* **2017**, *117* (10), 7190−7239.
(43) Schmidt, F.; Schönhoff, M. Solvate Cation Migration and Ion Correlations in Solvate Ionic Liquids. *J. Phys. Chem. B* **2020**, *124* (7), 1245−1252.
(44) Wohde, F.; Balabajew, M.; Roling, B. Li+Transference Numbers in Liquid Electrolytes Obtained by Very-Low-Frequency Impedance Spectroscopy at Variable Electrode Distances. *J. Electrochem. Soc.* **2016**, *163* (5), A714−A721.
(45) Dong, D.; Sälzer, F.; Roling, B.; Bedrov, D. How efficient is Li+ ion transport in solvate ionic liquids under anion-blocking conditions in a battery? *Phys. Chem. Chem. Phys.* **2018**, *20* (46), 29174−29183.
(46) Onsager, L. Reciprocal Relations in Irreversible Processes. I. *Phys. Rev.* **1931**, *37* (4), 405−426.
(47) Onsager, L. Reciprocal Relations in Irreversible Processes. II. *Phys. Rev.* **1931**, *38* (12), 2265−2279.
(48) Vargas-Barbosa, N. M.; Roling, B. Dynamic Ion Correlations in Solid and Liquid Electrolytes: How Do They Affect Charge and Mass Transport? *ChemElectroChem.* **2020**, *7* (2), 367−385.
(49) Suo, L.; Borodin, O.; Gao, T.; Olguin, M.; Ho, J.; Fan, X.; Luo, C.; Wang, C.; Xu, K. "Water-in-salt" electrolyte enables high-voltage aqueous lithium-ion chemistries. *Science* **2015**, *350* (6263), 938−943.
(50) Rangasamy, V. S.; Thayumanasundaram, S.; Locquet, J.-P. Solid polymer electrolytes with poly(vinyl alcohol) and piperidinium based ionic liquid for Li-ion batteries. *Solid State Ionics* **2019**, *333*, 76−82.

https://doi.org/10.1021/acsenergylett.3c00454
ACS Energy Lett. 2023, 8, 1944−1951